

Density functional investigation of the adsorption of a methane monolayer on an MgO(100) surface

Michael L. Drummond,¹ Bobby G. Sumpter,¹ William A. Shelton,¹ and J. Z. Larese^{2,3}

¹Computer Science and Mathematics Division, Oak Ridge National Laboratory, Oak Ridge, Tennessee 37831, USA

²Chemical Sciences Division, Oak Ridge National Laboratory, Oak Ridge, Tennessee 37831, USA

³Chemistry Department, University of Tennessee, Knoxville, Tennessee 37996-1600, USA

(Received 4 October 2005; published 15 May 2006)

The adsorption of a monolayer of methane upon the (100) surface of MgO was studied using a first-principles-based density functional approach employing a plane-wave basis set and periodic boundary conditions. Adsorption at both magnesium and oxygen sites was investigated, as were methane orientations where one, two, or three hydrogen atoms point toward the surface plane. In addition, the effect of one methane molecule on its neighbors was investigated by considering arrangements where translational symmetry across the surface was accompanied by appropriate rotations of the methane molecule. The minimum-energy configuration has the methane molecules located directly above a surface magnesium atom, the principal axis of the C_{2v} molecule is normal to the surface plane, and pairs of hydrogen atoms are oriented along the lattice lines that include adjacent (surface) oxygen atoms. Furthermore, neighboring methane molecules are rotated by 90° to reduce the H-H steric interactions. This arrangement has direct ramifications for the stability of other proposed, similar arrangements.

DOI: [10.1103/PhysRevB.73.195313](https://doi.org/10.1103/PhysRevB.73.195313)

PACS number(s): 68.43.Bc, 68.43.Fg, 68.47.Gh, 68.08.De

I. INTRODUCTION

The interaction of discrete molecules with the surface of an extended solid is an area of tremendously active research, being of importance to phenomena such as catalysis, corrosion, electronics, and adhesion. The first of these areas is especially relevant with respect to MgO, as it can function as either a support or an active catalyst in the crucially important oxidative coupling of methane to form longer hydrocarbons.¹ Although this particular reaction requires surface defects and irregularities,² MgO is nevertheless often considered a prototype for the metal oxide surface, which is of interest in the framework of heterogeneous catalysis.³ Furthermore, the square MgO(100) surface lattice offers a complementary alternative to the more frequently studied hexagonal surface lattice of graphite and close-packed metals. With respect to adsorbates, methane can be considered the most basic example of a hydrocarbon, and it is therefore no surprise that the combination of these two model systems has been the subject of a great deal of work.

Experimentally, the first investigation of the adsorption properties of methane on MgO was performed by Coulomb *et al.*, who used neutron diffraction to characterize the structure of deuterated methane on the MgO(100) surface.⁴ These studies suggested that CD₄, at both monolayer and bilayer coverages, formed a square lattice solid commensurate with the surface lattice, in contrast to the hexagonal close-packed lattice assumed for a monolayer of CH₄ above a graphite surface.⁵ The question of orientation of the methane molecules, a central theme of this current paper, was raised, but the diffraction data was not sufficiently precise to unequivocally differentiate between the possible options (e.g., free rotor, dipod, tripod, etc.; see Fig. 1). Subsequent He atom scattering studies and accompanying calculated binding energies were also inconclusive, although the face-down [Fig.

1(c), tripod] configuration of methane was deemed unlikely.⁶ Quasielastic neutron scattering has also been employed to study rotational diffusion of an adsorbed methane monolayer.⁷ Based on temperature-dependent studies, CH₄ was thought to rotate freely above 40 K, and assume either a free rotor or an edge-down [Fig. 1(b), dipod] orientation at lower temperatures; again the face-down configuration was considered to be inconsistent with the data. Finally, a great deal of experimental work has been performed by one of us (J.Z.L.), wherein neutron diffraction and inelastic neutron scattering was utilized to probe the rotational tunneling dynamics of adsorbed methane.⁸⁻¹² These studies indicated that a monolayer film forms a commensurate solid where the molecules assume the dipod orientation at temperatures below 15 K. Above 20 K, the molecules are found to be rotationally disordered, and melting occurs at 80 K.

Concurrent with the aforementioned experimental studies, a variety of theoretical methods have been applied to address the question of the orientation of adsorbed methane. In 1987,¹³ the Hartree-Fock electronic structure technique was used on three model systems: (1) a single CH₄ molecule on a

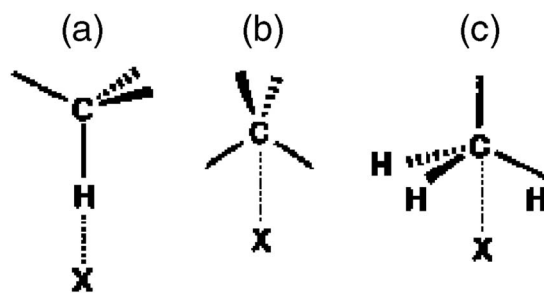


FIG. 1. Possible arrangements for CH₄ adsorbed on the surface (X=Mg or O). (a) Monopod orientation. (b) Dipod or edge-down orientation. (c) Tripod or face-down orientation.

surface represented by point charges, (2) a cluster of $\text{CH}_4\text{O}_4\text{Mg}_4$, and (3) four CH_4 molecules above a point-charge surface. The findings suggested the dipod orientation above Mg as the most stable, with the monopod arrangement being somewhat less stable and the tripod geometry much less stable. However, with respect to the simulation of the monolayer (model 3 above), the relative orientation of the methane molecules with respect to each other was beyond the precision of the method. The same year, calculations based on semiempirical potential energy models were performed,¹⁴ which were subsequently refined and improved over the years.^{15–17} Although the details of implementation and results differ, all such studies agree that the most stable arrangement is a tripod over Mg. Density functional calculations on model clusters (Mg_5O_5 and $\text{Mg}_{12}\text{O}_{12}$) found that CH_4 failed to adsorb to the (100) surface entirely,¹⁸ whereas more recent Hartree-Fock calculations^{19,20} support an assignment of a dipod adsorption of methane.

At this point, the literature seems to suggest accord about methane orientation within a given technique (e.g., neutron scattering favors dipod, potential energy calculations suggest tripod, *ab initio* calculations recommend dipod), but an overall consensus has proven elusive. In the current study, we use the computational technique of density functional theory (DFT), which has long been accepted as a robust method for solid-state investigations. The particular implementation of DFT used features the use of a plane-wave basis set, which can be adjusted to ensure an essentially complete basis. Moreover, the use of periodic boundary conditions avoids the necessity of employing point charges of somewhat arbitrary magnitude to model the MgO surface, and also obviates the need to approximate the system with a model of finite (and often small) size. Finally, the advances in computer efficiency that have occurred since the previous DFT work¹⁸ enable the current study to address questions not only about surface- CH_4 interactions, but also about CH_4 - CH_4 interactions. Thus, the calculations discussed below should be able to provide much deeper, and much more reliable, insight about the MgO- CH_4 system compared to previous efforts.

The paper is organized as follows. Section II describes the DFT methodology used. Section III then discusses the effects of varying the MgO(100) surface, and the details of both surface-adsorbate and adsorbate-adsorbate interactions. Finally, Sec. IV offers summary remarks and notes opportunities for future work.

II. COMPUTATIONAL METHODOLOGY

Nearly all calculations were performed using the periodic DFT program Vienna *ab initio* simulation package (VASP), version 4.6.6.²¹ The Kohn-Sham equations have been solved using the projector augmented wave (PAW) approach²² and a plane-wave basis set. The generalized-gradient approximation exchange-correlation functional of Perdew and Wang (PW91) was utilized.²³ Although it is well known that DFT underestimates binding that arises from dispersion effects, there is perhaps some indication that PW91 is a better choice for these systems than are other functionals available in VASP.²⁴ Moreover, as this paper is concerned with relative

stabilities rather than absolute values, and as all systems investigated are found to be bound, the use of PW91 seems justified. The Brillouin zone was sampled using an automated Monkhorst-Pack²⁵ scheme at a k -point sampling mesh of either 4×4 or 8×8 in the periodic directions, depending on the size of the supercell; the linear tetrahedron model with Blöchl corrections²⁶ was used to determine partial occupancies for each wave function. A plane wave energy cutoff of 600 eV was used, which should ensure an essentially complete basis set. The keyword `PREC=ACCURATE` was invoked, in order to minimize so-called “wrap around” errors and to ensure convergence of absolute energies to within a few meV. The electronic self-consistent field was deemed converged if the total energy between successive iterations differed by less than 10^{-5} eV/atom; similarly, geometries were deemed converged if an optimization step resulted in an energy within 10^{-4} eV/atom of the previous optimization step. Geometries were optimized using a conjugate gradient algorithm. Symmetry constraints were not utilized, to ensure maximum degrees of freedom. All other parameters were left at their default values.

In order to investigate the MgO/ CH_4 interface, the slab approach was utilized. In VASP, a cell is periodic in three dimensions. While this translation is desirable along the MgO(100) plane, it is certainly unphysical in the direction perpendicular to the surface. To avoid interactions in this direction, a vacuum thickness of at least 10 Å was incorporated into the calculation; ensuring at least 15 Å difference was found to have a negligible effect on the accuracy of the calculation. MgO crystallizes into the rock salt structure ($B1$, $Fm\bar{3}m$), and so a six-layer slab was defined for most calculations. A three-layer slab was used for certain larger supercells (see below) to ensure computational expediency. Details about the lattice parameters used are given below.

A few calculations of finite MgO clusters with adsorbed CH_4 were performed using the Amsterdam density functional (ADF) program.²⁷ The PW91 exchange and correlation functional was again used, in conjunction with a basis set of double- ζ size and augmented with one set of polarization functions. The frozen core approximation was used for all 1s electrons on nonhydrogen atoms. All convergence criteria were left at their default values.

III. RESULTS AND DISCUSSION

A. Effect of surface geometry

One of the main reasons for investigating the adsorption of CH_4 on MgO is the similarity in their lattice parameters (4.18 Å in the former²⁸ and 4.21 Å in the latter²⁹), which drives methane to adopt a square lattice commensurate with the surface structure. Optimization of the lattice parameter for bulk MgO (i.e., without adsorbed methane) using PW91 results in a value of 4.25 Å, reasonably close to the experimental value but less in line with the lattice parameter for solid methane. As a result, the total energy of the combined MgO/ CH_4 system is actually lower when the experimental MgO lattice parameter of 4.21 Å is used, presumably owing to the fact that it is more commensurate with the preferred

TABLE I. Relative energies and methane to surface distances for six arrangements of CH_4 above the $\text{MgO}(100)$ surface.

System	Relative Energy (meV)	Mg- or O-to-C distance (\AA)
C_{2v} -Mg	0	3.250
$C_{3v}(1)$ -O	6.32	3.506
C_{2v} -O	6.53	3.795
$C_{3v}(3)$ -Mg	10.66	3.254
$C_{3v}(3)$ -O	24.85	3.549
$C_{3v}(1)$ -Mg	30.57	3.689

spacing of CH_4 molecules. In addition, calculations of the barrier to rotate a methane molecule about an axis perpendicular to the surface, which will be discussed in detail elsewhere, are largely unaffected by the choice of MgO lattice constant, be it calculated or experimentally determined. Therefore, the optimized lattice parameter of isolated MgO was not used.

In order to further refine the optimum description of the MgO lattice in the presence of adsorbed CH_4 , three calculations were performed: (1) three layers of MgO were allowed to freely optimize over three layers frozen at the experimental value; (2) three layers of MgO were optimized over five constrained experimental layers; and (3) four layers of MgO were optimized over four experimental layers. The carbon-to-surface distances were fairly constant in all three simulations (3.208, 3.214, and 3.206 \AA , respectively). Furthermore, as before, the barriers to rotation for a CH_4 molecule proved insensitive to the optimization of surface atoms. Thus, for the sake of computational expediency and consistency, the experimental lattice constant of MgO of 4.21 \AA was used for all calculations described below.

B. Effect of CH_4 orientation

As mentioned in the Introduction, there is a great deal of often contradictory data concerning the manner in which methane binds to the MgO surface. In particular, two especially relevant questions are whether one, two, or three hydrogens are oriented toward the surface [denoted $C_{3v}(1)$, C_{2v} , and $C_{3v}(3)$ in this study; see Fig. 1], and whether CH_4 preferentially occupies a site above a magnesium or above an oxygen (indicated by either a -Mg or an -O after the CH_4 symmetry labels given above). Preliminary calculations at the semiempirical level (not shown) suggested that bridge and hollow sites are disfavored with respect to on-top binding, and thus they will not be discussed. Table I presents the relative total energies for supercells consisting of adsorbed methane and a six-layer MgO slab (for a total of 12 magnesium and 12 oxygen atoms). Each of these supercells measures $4.21 \times 4.21 \times 25 \text{\AA}^3$ and is described with a k -point grid (see above) of $8 \times 8 \times 1$. In addition, the distance between the nearest surface atom and the methane carbon is also given.

In accord with previous Hartree-Fock studies,^{13,19,20} the dipod-down CH_4 adsorbed commensurately above Mg (C_{2v} -Mg) was found to be the most stable configuration in

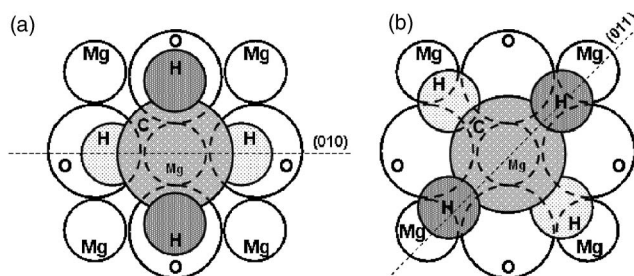


FIG. 2. Top-down view of two possible orientations of one C_{2v} -Mg methane molecule adsorbed to the $\text{MgO}(100)$ surface. (a) Oriented along the (010) axis. (b) Oriented along the (011) axis. The shaded circles are the adsorbed species, with decreasing darkness indicating increased proximity to the unshaded surface.

the current investigation. Moreover, such an arrangement is consistent with the bulk of the experimental data mentioned earlier, although most such identifications were accompanied by appropriate caveats. It should be noted, however, that the fully quantum-mechanical treatment employed in this study contradicts the conclusions of the semiempirically based pair potential approaches,¹⁴⁻¹⁷ which universally favor the $C_{3v}(3)$ -Mg arrangement. More surprisingly, all six possible arrangements are found to be stable, in contrast to an earlier DFT calculation,¹⁸ which found no adsorption whatsoever. Given that the Becke-Perdew 1986 functional³⁰ employed in the earlier work is similar to the PW91 functional used in this work, both employing the so-called generalized-gradient approximation, and further given that the earlier employed basis set is of a reasonable size, it is likely that the periodic boundary conditions applied in the current work account for the discrepancy. Taking advantage of the putative translational symmetry of the surface-adsorbate system evidently provides a description more in accord with experiment than does the truncated model cluster of Mg_5O_5 .

Evidence to support the necessity of a large cluster for an accurate depiction was provided through finite cluster calculations on $\text{Mg}_{64}\text{O}_{64}\text{-CH}_4$ (i.e., two square slabs of MgO , each measuring eight atoms per side, with a single adsorbed methane molecule). Although the details of relative stability and surface-to-methane distances vary somewhat from the periodic results discussed earlier, the picture is generally the same, and all of the arrangements in Table I are stationary structures. The ramifications on the necessity of accurate, periodic calculations, such as those in this study, will likely continue to manifest themselves in similar investigations in the future. However, at the present time, this paper will focus on the periodic calculations, which avoid truncation issues.

One final aspect of adsorbate orientation concerns the direction in which the hydrogen atoms point. For the C_{2v} structures, the two likely orientations are along the (010) surface axis [Fig. 2(a)] or along the (011) surface axis [Fig. 2(b)]. Similar arrangements can be envisioned for the C_{3v} structures. In order to investigate this effect, the optimization of the methane molecule was begun with at least one hydrogen (two for the C_{2v} structures) along the (010) axis. Once this structure converged, the methane was rotated (without subsequent reoptimization) in 15° increments about the axis perpendicular to the MgO surface, up to 90° for the C_{2v} struc-

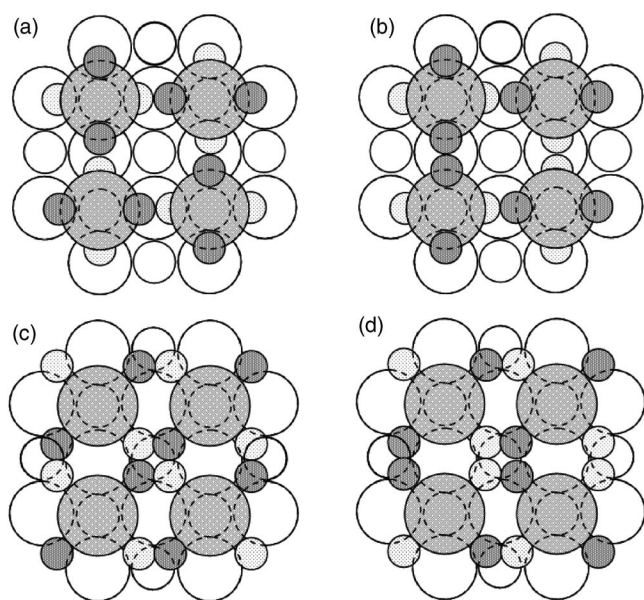


FIG. 3. Four possible orientations of methane adsorbed above a MgO(100) surface. The circle colors and sizes correspond to those defined in Fig. 2.

tures and up to 60° for the C_{3v} structures. If the resulting energy vs angle of rotation plot did not have a minimum at the originally optimized structure, the position of the CH_4 was reoptimized starting from the orientation of the minimum along the energy-angle plot. This process was performed recursively until the optimized structure was found to be a minimum with respect to rotation. Most of the structures in Table I have their minima in orientations along the (010) axis; the exception is $C_{2v}\text{-O}$, where the methane is oriented along the (011) axis. However, as will be discussed below, it is unlikely that any of the structures in Table I represent global minima, due to neighboring $\text{CH}_4\text{-CH}_4$ interactions.

C. Effect of $\text{CH}_4\text{-CH}_4$ Interactions

The structures in Table I were determined with one CH_4 per supercell, with identical orientations of the CH_4 translated along the crystallographic a and b axes. Yet it is also possible—and indeed, as will be shown, likely—that the methane molecules do not possess such rigorous translation symmetry. Conceptually, it is unlikely that mixtures of C_{2v} , $C_{3v}(1)$, and $C_{3v}(3)$ orientations are found on the same monolayer, as they cannot pack together efficiently. However, it is much more appealing, at least to a first approximation, to envision translation symmetry along a monolayer being broken by having a methane rotated with respect to its neighbor (or neighbors). Figure 3 depicts some possibilities along these lines starting with the motif of the minimum energy structure of Table I, $C_{2v}\text{-Mg}$.

Explicit calculations have been performed for the arrangements depicted in Fig. 3. For these structures, four methane molecules are present in each supercell, in contrast to the one methane per supercell of the previous section, in order to explicitly vary the interactions between neighboring CH_4 molecules. As these supercells are four times larger than

TABLE II. Relative energies and methane-to-surface distances for five arrangements of C_{2v} methane above Mg.

System	Relative energy (meV)	Average Mg-to-C distance (Å)
Figure 3(a)	0	3.261
Figure 3(b)	24.37	3.268
Figure 3(c)	42.59	3.365
Figure 3(d)	42.96	3.392
$C_{2v}\text{-Mg}$	51.63	3.250

those previously described, measuring $8.42 \times 8.42 \times 25 \text{ \AA}^3$, the k -point grid was reduced to a $4 \times 4 \times 1$ description, and the MgO slab thickness was reduced from six layers to three, for the sake of computational expediency. The results of these larger calculations are presented in Table II. Also shown in Table II, for the sake of comparison, is a similar calculation based on the $C_{2v}\text{-Mg}$ structure of Table I, where each methane molecule possesses the same orientation as its neighbors.

It is obvious from Fig. 3 and Table II that varying the rotational orientation from methane to methane has a tremendous effect, as all of these arrangements are lower in energy than the lowest-energy structure of Table I. Overall, the lowest-energy structure is that shown in Fig. 3(a), where neighboring methane atoms are rotated 90° with respect to each other. The increased stability of Fig. 3(a) with respect to $C_{2v}\text{-Mg}$ cannot be accounted for by invoking differences in the interactions with the MgO surface, as the methane molecules in Fig. 3(a) are actually slightly (0.01 \AA) further from the surface. Instead, the explanation clearly involves an amelioration of neighboring H-H steric interactions by rotation. For example, in $C_{2v}\text{-Mg}$, the nearest-neighbor H-H distance is 2.42 \AA , whereas this distance is significantly increased to 2.72 \AA in the structure in Fig. 3(a). Figure 3(b), where rotation from neighbor to neighbor occurs along only one crystallographic axis, shows both of the aforementioned nearest-neighbor distances. In Fig. 3(c), this distance actually *increases* substantially, to 3.20 \AA , yet this structure is less stable than those of Figs. 3(a) and 3(b), presumably because each hydrogen in Fig. 3(c) has two nearest-neighbor interactions. Figure 3(d), as expected based on this line of reasoning, is the least stable of the structures depicted in Fig. 3.

These considerations render unnecessary similar calculations on the C_{3v} systems described in Table I, despite the fact that one such structure, a $C_{3v}(3)\text{-Mg}$ -based structure with appropriate rotations between neighboring methanes, was previously determined to be the optimum arrangement.¹⁵ As mentioned earlier, for $C_{2v}\text{-Mg}$, the nearest neighbor H-H distance is 2.42 \AA , and there are of course four of these interactions per CH_4 . In contrast, for any C_{3v} structure, there are only three nearest neighbor H-H interactions, as the fourth hydrogen atom points either towards the surface or away from it, for the monopod and tripod cases, respectively. The three H-H distances for $C_{3v}(3)\text{-Mg}$ are 2.423 \AA , similar to the distance in $C_{2v}\text{-Mg}$, and 2.791 and 2.825 \AA , which are much longer distances. Thus, even though there is significantly less H-H steric interaction in the $C_{3v}(3)\text{-Mg}$ arrange-

ment as compared to C_{2v} -Mg, the former structure is still 10.66 meV less stable than the latter. Identical arguments hold true for the other C_{3v} structures of Table I, and the case against a rotated C_{2v} -O being the optimum arrangement similarly makes itself. Therefore, based on the results of the present calculational approach, methane adsorbs to the (100) face of MgO with the arrangement shown in Fig. 3(a).

As a final test of both the assignment of Fig. 3(a) as the minimum-energy structure and the influence of steric hinderance in making it so, structures with 3/4 monolayer coverages were also investigated for the structural motifs given in Table II. As is the case with the full monolayer structure, the arrangement depicted in Fig. 3(a) is the lowest-energy structure, thereby cementing the status of this geometry as the likely global minimum. Similarly, the structure of Fig. 3(b) is the next most stable, although the difference in stability is much smaller than for the full monolayer coverage (8.44 vs 24.37 meV, respectively). None of the geometries for the 3/4 monolayer coverages differ substantially from their corresponding full monolayer counterparts—that is, both the surface-to-methane distances in Table II and the H-H distances described above are consistent to within 0.002 Å. Thus, it is evident that the decrease in the number of nearest-neighbor H-H interactions is responsible for the smaller energy gap between the structures in Figs. 3(a) and 3(b).

However, in contrast to the findings shown in Table II, the structures in Figs. 3(c) and 3(d) are actually higher in energy than unrotated C_{2v} -Mg at 3/4 monolayer coverage. It seems logical to conclude that, whereas nearest-neighbor H-H interactions are the primary arbiter of stability at the full monolayer, at 3/4 monolayer, surface-methane interactions are responsible for the relative stability of the structures in Figs. 3(a), 3(b), and C_{2v} -Mg compared to those in Figs. 3(c) and 3(d). In other words, at 3/4 monolayer (and presumably lower) coverages, structures where the methane hydrogens point toward a surface oxygen are favored, with steric hinderance determining the relative stabilities of all geometries satisfying this initial requirement. In contrast, at full coverage, the steric hinderance argument takes precedence over the arrangement of the methane molecules with respect to neighboring oxygen atoms. This balance is typical of the competition between surface-adsorbate and adsorbate-adsorbate interactions, which is well known.

IV. CONCLUSIONS AND FUTURE WORK

In order to complement a wealth of somewhat ambiguous or even contradictory experimental work, and also in order to

augment extant calculations with higher-quality results, a first-principles-based DFT study of the adsorption of CH_4 onto the MgO(100) surface was performed. It was quickly revealed that CH_4 preferentially adsorbs directly above a magnesium atom in an edge-down, or dipod, fashion, forming a methane monolayer commensurate with the substrate. Furthermore, the layer arranges in a manner where each C_{2v} methane molecule is rotated 90° with respect to its four methane neighbors. As a result of this arrangement, the H-H distances between neighboring methanes increase, thereby reducing steric hinderance. While similar phenomena presumably operate in monolayer arrangements of C_{3v} methane, calculations reveal that these systems experience less steric hinderance than do similar packings of C_{2v} methane, and yet the former methane orientation is still less energetically stable than the latter. Moreover, calculations with 3/4 monolayer coverages also prefer this same structural motif, although the balance between surface-adsorbate and adsorbate-adsorbate interactions complicates the picture somewhat. Regardless, it is with confidence that we put forth the structure in Fig. 3(a) as the optimum arrangement for a methane monolayer on the (100) surface of MgO.

Subsequent work utilizing both new computational approaches and recent experimental data will serve to either cement this proposed arrangement or point toward an alternative. For example, work is in progress to compare experimental inelastic neutron scattering tunneling spectra with plots of neutron energy loss vs $S(Q, \omega)$ calculated from vibrational data.³¹ In addition, studies similar to the current work have already begun to investigate the effects of adding more layers above the monolayer investigated herein. These studies, in particular the changes that manifest during layer-by-layer growth,³² are also particularly well suited for comparison to experiment, and will also provide an even more stringent test for the applicability of DFT to study adsorbates weakly bound to a surface.

ACKNOWLEDGMENTS

The research was sponsored by Division of Materials Science of Oak Ridge National Laboratory (ORNL), U.S. Department of Energy under Contract No. DE-AC05-00OR22725 with UT-Battelle, LLC at ORNL. The extensive computations were performed using the resources of the National Center for Computational Sciences at ORNL.

¹J. H. Lunsford, *Angew. Chem., Int. Ed. Engl.* **34**, 970 (1995).

²K. J. Klabunde and I. Nieves, *J. Phys. Chem.* **92**, 2521 (1988).

³J. M. Thomas and W. J. Thomas, *Principles and Practice of Heterogeneous Catalysis* (VCH, Weinheim, Germany, 1997).

⁴J. P. Coulomb, K. Madih, B. Croset, and H. J. Lauter, *Phys. Rev. Lett.* **54**, 1536 (1985).

⁵P. Vora, S. K. Sinha, and R. K. Crawford, *Phys. Rev. Lett.* **43**, 704 (1979).

⁶D. R. Jung, J. Cui, D. R. Frankl, G. Ihm, H.-Y. Kim, and M. W. Cole, *Phys. Rev. B* **40**, 11893 (1989).

⁷J. M. Gay, P. Stocker, D. Degenhardt, and H. J. Lauter, *Phys. Rev. B* **46**, 1195 (1992).

⁸J. Z. Larese, J. M. Hastings, L. Passell, D. Smith, and D. Richter, *J. Chem. Phys.* **95**, 6997 (1991).

⁹J. Z. Larese, B. Asmussen, M. A. Adams, C. Carlile, D. Martin, and M. Ferrand, *Physica B* **226**, 221 (1996).

- ¹⁰J. Z. Larese, *Physica B* **248**, 297 (1998).
- ¹¹J. Z. Larese, D. M. y Marero, D. S. Sivia, and C. J. Carlile, *Phys. Rev. Lett.* **87**, 206102 (2001).
- ¹²T. Arnold, R. Cook, D. Martin, M. A. Adams, and J. Z. Larese, *Isis* **8**, 19 (2003).
- ¹³B. Deprick and A. Julg, *New J. Chem.* **11**, 299 (1987).
- ¹⁴C. Girard and C. Girardet, *Chem. Phys. Lett.* **138**, 83 (1987).
- ¹⁵A. Alavi, *Mol. Phys.* **71**, 1173 (1990).
- ¹⁶A. Lakhlifi and C. Girardet, *Surf. Sci.* **241**, 400 (1991).
- ¹⁷S. Picaud, C. Girardet, T. Duhoo, and D. Lemoine, *Phys. Rev. B* **60**, 8333 (1999).
- ¹⁸A. M. Ferrari, S. Huber, H. Knözinger, K. M. Neyman, and N. Rösch, *J. Phys. Chem. B* **102**, 4548 (1998).
- ¹⁹K. Todnem, K. J. Børve, and M. Nygren, *Surf. Sci.* **421**, 296 (1999).
- ²⁰M. Lintuluoto and Y. Nakamura, *J. Mol. Struct.: THEOCHEM* **674**, 207 (2004).
- ²¹G. Kresse and J. Hafner, *Phys. Rev. B* **47**, 558 (1993); **49**, 14251 (1994); G. Kresse and J. Furthmüller, *Comput. Mater. Sci.* **6**, 15 (1996); *Phys. Rev. B* **54**, 11169 (1996).
- ²²P. E. Blöchl, *Phys. Rev. B* **50**, 17953 (1994); G. Kresse and D. Joubert, *ibid.* **59**, 1758 (1999).
- ²³J. P. Perdew, J. A. Chevary, S. H. Vosko, K. A. Jackson, M. R. Pederson, D. J. Singh, and C. Fiolhais, *Phys. Rev. B* **46**, 6671 (1992); **48**, 4978 (1993).
- ²⁴J. Langlet, J. Bergès, and P. Reinhardy, *Chem. Phys. Lett.* **396**, 10 (2004).
- ²⁵H. J. Monkhorst and J. D. Pack, *Phys. Rev. B* **13**, 5188 (1976).
- ²⁶P. E. Blöchl, O. Jepsen, and O. K. Andersen, *Phys. Rev. B* **49**, 16223 (1994).
- ²⁷G. te Velde, F. M. Bickelhaupt, S. J. A. van Gisbergen, C. Fonseca-Guerra, E. J. Baerends, J. G. Snijders, and T. Ziegler, *J. Comput. Chem.* **22**, 931 (2001); C. Fonseca-Guerra, J. G. Snijders, G. te Velde, and E. J. Baerends, *Theor. Chem. Acc.* **99**, 391 (1998); ADF2005.01, SCM, Theoretical Chemistry, Vrije Universiteit, Amsterdam, The Netherlands, <http://www.scm.com>.
- ²⁸W. Press, *J. Chem. Phys.* **56**, 2597 (1972).
- ²⁹Inorganic Index to Powder Diffraction File (Joint Committee on Powder Diffraction Standards, International Center for Powder Diffraction Data, Swarthmore, PA, 1997, MgO—Card No. 04–0820).
- ³⁰A. D. Becke, *Phys. Rev. A* **38**, 3098 (1988); J. P. Perdew, *Phys. Rev. B* **33**, 8822 (1986); **34**, 7406 (1986).
- ³¹A. J. Ramirez-Cuesta, *Comput. Phys. Commun.* **157**, 226 (2004).
- ³²A. Freitag and J. Z. Larese, *Phys. Rev. B* **62**, 8360 (2000).